Available online at www.sciencedirect.com
SCIENCE DIRECT®
Icarus 170 (2004) 430–442
ICARUS
www.elsevier.com/locate/icarus

Io's volcanic control of Jupiter's extended neutral clouds

Michael Mendillo [a,*], Jody Wilson [a], John Spencer [b], John Stansberry [c]

[a] *Center for Space Physics, Boston University, 725 Commonwealth Avenue, Boston, MA 02215, USA*
[b] *Lowell Observatory, Flagstaff, AZ 86001, USA*
[c] *University of Arizona, Steward Observatory, Tucson, AZ 85721, USA*

Received 12 December 2002; revised 3 January 2004

Available online 9 June 2004

Abstract

Dramatic changes in the brightness and shape of Jupiter's extended sodium nebula are found to be correlated with the infrared emission brightness of Io. Previous imaging and modeling studies have shown that varying appearances of the nebula correspond to changes in the rate and the type of loss mechanism for atmospheric escape from Io. Similarly, previous IR observational studies have assumed that enhancements in infrared emissions from Io correspond to increased levels of volcanic (lava flow) activity. In linking these processes observationally and statistically, we conclude that silicate volcanism on Io controls both the rate and the means by which sodium escapes from Io's atmosphere. During active periods, molecules containing sodium become an important transient in Io's upper atmosphere, and subsequent photochemistry and molecular-ion driven dynamics enhance the high speed sodium population, leading to the brightest nebulas observed. This is not the case during volcanically quiet times when omni-present atmospheric sputtering ejects sodium to form a modest, base-level nebula. Sodium's role as a "trace gas" of the more abundant species of sulfur (S) and oxygen (O) is less certain during volcanic episodes. While we suggest that volcanism must also affect the escape rates of S and O, and consequently their extended neutral clouds, the different roles played by lava and plume sources for non-sodium species are far too uncertain to make definitive comparisons at this time.

Keywords: Io; Jupiter, magnetosphere; Satellites, atmospheres; Volcanism

1. Introduction

Jupiter's magnetosphere offers one of the richest blends of geological, atmospheric, and space plasma physics phenomena in the Solar System. The heavy ions of oxygen and sulfur which dominate the mass and energy budget of the magnetosphere have their origin in the volcanoes of Jupiter's remarkable moon, Io. From the volcanoes, the sulfur and oxygen move by steps into Io's atmosphere and onto its surface, and then into large extended neutral clouds around Io and Jupiter via atmospheric escape. By subsequent ionization and pickup they populate the plasma torus, and finally they exit the jovian system altogether by outward diffusion, charge exchange reactions, or by precipitation into Jupiter's auroral regions.

Several spacecraft encounters with Jupiter—Pioneer in 1973–1974, Voyager in 1979, and Ulysses in 1992—have provided snapshots of the jovian magnetospheric environment. These remarkable datasets provided insights into a complex system of volcanism, surface geology, atmospheres, charged particles and fields. On a much longer multi-year timescale, the Galileo satellite has just completed a detailed in-situ study of variations of Io, the plasma torus, and the magnetosphere as a whole. Complementing these spacecraft missions to Jupiter has been an ongoing series of observations conducted from the ground and from low-Earth-orbit. We describe here a decade long view of changes in the jovian sodium nebula and contemporaneous observations of volcanic activity on Io.

The sodium clouds generated by Jupiter's satellite Io provide a window through which to examine a complex chain of processes that appear to dominate a magnetosphere in a way not found elsewhere in the Solar System. While a consensus model is far from complete, its potential elements have been described in several review articles (Schneider et al., 1989; Spencer and Schneider, 1996; Thomas, 1997; Bagenal, 2004). Briefly, volcanic eruptions of lava and geyser-like plumes populate its surface and atmosphere with

* Corresponding author. Fax: 617-353-6463.
E-mail address: mendillo@bu.edu (M. Mendillo).

0019-1035/$ – see front matter
doi:10.1016/j.icarus.2004.03.009

several gases (SO_2, SO, S, O); a minor species is sodium, important for its easy detection at visible wavelengths and thus as a "tracer" of the more plentiful elements. Energetic ions trapped in Jupiter's magnetic field bombard the atmosphere and the surface of Io, "sputtering" some of the Na atoms off of Io and into orbits around Jupiter. Some of the atmospheric gases still bound to Io and others in near-Io orbits about Jupiter become ionized by the impact of energetic plasmas and solar EUV radiation. These low energy plasmas are subject to Jupiter's strong, corotating magnetic field, and thus magnetic capture (or "pick-up") leads to the maintenance of a plasma torus surrounding the planet at approximately the radial distance of Io ($5.9R_J$), as well as an ionosphere on Io.

Recycling of plasma back into the neutral gas state involves an equally remarkable series of steps linked to the fact that three distinct populations co-exist near Io: torus plasma traveling at co-rotational speeds ($\sim$ 75 km/sec), together with neutrals and ionospheric plasma moving with Io's orbital speed ($\sim$ 17 km/sec). Neutralizations of the atomic and molecular ions near Io or in the plasma torus result in the release of neutral sodium at high speeds (Na^*) sufficient to escape from the magnetosphere, essentially unaffected by any other process, to form a great nebula. Within this giant structure, the slower speed, sputtered sodium (Na) forms the elongated cloud that orbits Jupiter with Io (the "banana" cloud).

There is a rich literature relating to the individual sodium clouds composed of Na near Io and Na^* forming jets, streams and nebulas. Using images of the Io sodium clouds at multiple fields of view ($\pm 7R_J$, $\pm 30R_J$, $\pm 500R_J$) from 1990–1996, (Wilson et al., 2002) formulated a working model of the overall jovian sodium budget. They determined that various combinations of two basic atmospheric escape processes—atmospheric sputtering of Na, and ionospheric escape of an unidentified molecular sodium ion (NaX^+)—are needed to explain essentially all manifestations of the sodium clouds. The pick-up of NaX^+ and its subsequent destruction in the torus to form a "stream" or distributed source of Na^* produces a bright and distinctly rectangular-shaped sodium nebula when it is the dominant process. Atmospheric sputtering may also contribute to the nebula, but its efficiency in doing so depends strongly on the velocity distribution of the escaping neutrals that result. Given a sufficient fraction of higher-speed ejections, atmospheric sputtering was shown to produce a faint and somewhat diamond-shaped nebula around Jupiter during times when it is not competing with NaX^+ escape. Simple charge exchange, once thought to be the dominant escape mechanism, is now understood to be only a minor exospheric process because it is unable alone to account for the appearances seen simultaneously in the three fields-of-view datasets. Thus, we are now at the stage where imaging observations of the sodium nebula provide a quantitative measure of both the rates and means of atmospheric escape from Io. The next step is to investigate how the coupled neutral–plasma system at $\sim 6R_J$ responds to changes in Io's volcanism.

2. Volcanic activity and the sodium nebula

Given the primary role of volcanic activity (lava flows and plumes) in producing Io's atmosphere, it is reasonable to expect that Io's sodium clouds and plasma torus should be affected by changes in Io's volcanism. Yet, no observational study to date has been able to demonstrate such a relationship. We address this issue here by presenting the first comparison of neutral sodium cloud data with contemporaneous measurements of volcanic activity over a nine-year period. The two main challenges are (1) finding measurements which somehow quantify "volcanic activity," and (2) given that sodium cloud observations and observations of volcanic activity rarely, if ever, occur on the same night, finding a way of estimating volcanic activity during a sodium cloud observation from the nearest volcanic observations available. These are difficult issues open to varying interpretations and thus detailed discussions are required.

2.1. Observations of sodium nebula

The distant Na^* atoms in the nebula were successfully imaged for the first time in December 1989 (Mendillo et al., 1990; Flynn et al., 1994) and at yearly intervals since then. The imaging technique used to observe Jupiter's sodium nebula has been described in several previous works (Mendillo et al., 1990; Baumgardner and Mendillo, 1993; Baumgardner et al., 1993). The basic approach is to use a small refractor (0.1 m aperture) to achieve a large field of view (approximately 6°), an interference filter (5893 ± 7 Å) to capture the $D_1 + D_2$ sodium lines, an occulting mask to prevent the bright image of Jupiter from reaching the detector, and a CCD camera (both image-intensified and bare version have been used over the past decade). On- and off-band sequences of on-target and off-target images are used to separate scattered light and terrestrial sodium from the jovian signal. Calibration to absolute brightness units is done using either a standard source or standard stars.

Observations of the sodium nebula have been made each year since its discovery. Optimal conditions require Jupiter near opposition, a moonless sky, and extremely clear and photometric atmospheric conditions. In most cases, such low brightness level imaging requirements occurred on one (or at best a few nights) of each observing season. Hence, while there is continuity of nebula observations from year to year, shorter time resolution issues cannot be addressed with such a dataset.

2.2. Observations of infrared emission

Observations of infrared (IR) emission from Io are taken to be a readily available measure of hot lava flows associated with volcanic activity. These observations can be made with groundbased telescopes, and it is even possible to distinguish individual points of emission, or "hotspots," representing particular volcanic features on Io. These types of

observations have been made far more frequently than imaging observations of volcanic plumes, the signature of volcanism that is a more direct injection of volcanic gases into Io's atmosphere. Thus, regardless of whether or not infrared emission is the best proxy for the volcanic contribution to Io's atmosphere, it provides by far the *best possibility* for correlation studies with the sodium clouds. A major issue, however, is that the patrol-type IR observations needed to monitor Io's volcanism are usually allotted telescope time on nights when the Moon is up, and thus the nebula and volcanic datasets are not often simultaneous; we address this by a careful analysis of statistical patterns and trends to arrive at the best possible indicator of volcanism for each nebula observation.

To obtain the best statistical comparisons possible, we select a dataset that (1) includes relatively frequent observations, (2) that is most representative of "overall volcanic activity," and (3) that is as consistent as possible over the time period from 1990 to 1998. The disk-averaged brightness of Io's Jupiter-facing hemisphere at 3.5 and 3.8 μm appears to be the best measure available. Io's Jupiter-facing hemisphere has been observed more frequently than other longitudes because it can be seen during eclipse when Io is in Jupiter's shadow, a time when sunlight does not strike Io's disk and contaminate the IR measurements. The 3.5- and 3.8-μm wavelengths are a middle-ground between the 2.2-μm band, whose brightness can change quickly at Io, and which is most sensitive to small, hot volcanoes, and the 4.8-μm band which varies more slowly, and which is more sensitive to large and relatively cool expanses of lava on Io's surface. Indeed, there have been periods of time when the 2.2-μm brightness of Io was many times greater than average, while the 4.8-μm brightness remained nearly unchanged, and vice-versa. We eliminate the problem of judging the volcanic activity level from Io from such disparate measurements by using the wavelengths in-between, where there is significant sensitivity to both extreme cases. For the few cases where data is not available at 3.5 or 3.8 μm, we use statistical arguments to estimate those brightnesses from 2.2- and 4.8-μm data, as discussed in the next section. For this study we incorporate a combination of published measurements (Spencer et al., 1992, 1994, 1997; Veeder et al., 1994; Howell and Klassen, private communication, 2002; Silverstone et al., 1995; Stansberry et al., 1997) and previously unpublished measurements obtained at NASA's Infrared Telescope Facility using NFSCAM.

2.3. Estimating volcanic activity levels during nebula observations

The available IR measurements are shown in Table 1, where they have been converted to the same units for ease of comparison.

The entries in Table 1 describe the remarkable accomplishment of "monitoring volcanism" on a tiny, remote world. Our analysis of this chronology of episodic activity led us to define the 3.5-μm brightness of 30 GW/(str μm) as the boundary between "bright" and "dim" values, corresponding to volcanically "active" and "quiet" states. Brightnesses tend to show periods of either slowly-changing values that are less than this cutoff, or more variable values greater than the cutoff, consistent with our interpretation of active and quiet periods. Thus, while the 30 GW/(str μm) choice appears to be somewhat arbitrary, our statistical analyses (described below and in an Appendix A) provide support for there being both unambiguous activity patterns per se for Io's volcanism, and that such a threshold level can be proposed.

The time sequence of volcanic activity on Io can be described as follows: The large volcano Loki erupted on a 540-day cycle during our years of study, with average eruptions lasting 230 days, and quiet periods lasting at least 150 days (Rathburn et al., 2002). Loki eruptions do not appear to be interrupted by any temporary quiet periods, nor are the lulls in-between eruptions interrupted by short-term Loki activity. Thus, Io is undoubtedly volcanically active on any day during a Loki eruption. The nebula observations of 1990, 1991, August 1997, and 1998 (both) were made during Loki eruptions.

On top of the Loki eruption cycle, the remainder of volcanic activity on Io is characterized by relatively short-duration eruptions separated by longer periods of quiescence. Except for Loki, Io is volcanically quiet for the majority of the time, as monitored by the IR techniques. Thus IR observations are critical during Loki lulls to determine the activity levels of the remaining volcanoes. The nebula of 1995 was observed during the quiet phase of the Loki cycle, but it also occurred during an eruption of one of the minor volcanoes, Tiermes Patera, which lasted between 60 and 80 days. IR observations showing high activity were made both before and after each of these nebula observations, meaning there is little doubt that the nebulas represent high volcanic activity levels.

Non-Loki eruptions have durations which are much shorter than a Loki eruption, anywhere from a few months to less than a day, so accurate determinations of non-Loki activity require frequent measurements. Thus, during Loki lulls, our knowledge of the total volcanic activity level of Io during a nebula observation is only as good as the available IR measurements taken on the same day or nearby days. Five nebulas were observed during lulls in the Loki cycle along with accompanying IR observations showing quiet levels. However, in most cases there are gaps of several days between the nebula and IR measurements, meaning short-term eruptions could have occurred during the nebula observations without being seen in IR. We therefore use our large dataset of IR observations to statistically characterize non-Loki eruptions, and then calculate the probability of eruptions happening during these nebula observations. Whenever possible, we make assumptions that maximize the possibility of volcanic activity during these nebula observations in the Loki lulls, making it as difficult as possible

Table 1
Infrared observations of Io's Jupiter-facing hemisphere

Date	IR brightness (GW/(str μm))				Ref.[a]	Long.	Active volc.
	2.3 μm	3.5 μm	3.8 μm	4.9 μm			
1989–1990							
11/24				240.0 ± 65.0	H	345	Loki (H)
12/15				103.0 ± 10.0	V	343	Loki
01/07				144.0 ± 14.0	V	332	Loki
01/09				241.0 ± 24.0	V	348	Loki +
01/25							(Nebula)
02/26				85.0 ± 8.0	H	15	Loki (H)
1990–1991							
10/12	4.3 ± 0.6		43.6 ± 6.5	68.3 ± 18.7	S94	345	
12/29		66.4 ± 9.8	115.0 ± 11.0		S94	345	Loki (S94)
01/12	22.3 ± 2.2		119.0 ± 11.0	178.0 ± 17.0	S94	345	Loki
2/7–18							(Nebula)
02/15	17.2 ± 2.5		93.1 ± 9.0	174.0 ± 35.0	S94	15	Loki
02/22	21.3 ± 3.2	70.6 ± 6.8	97.7 ± 9.4	132.0 ± 34.0	S94	15	Loki
03/17				120.0 ± 7.0	H	15	Loki
03/26	11.1 ± 1.1		79.7 ± 7.7	116.0 ± 17.0	S94	15	Loki (S94)
04/09		52.4 ± 4.0			S94	15	Loki
1991–1992							
10/31	7.2 ± 0.4		31.2 ± 1.8		S92	345	
11/07			36.2 ± 2.8	70.0 ± 10.0	S92	345	
12/09	4.1 ± 2.4	19.5 ± 1.1	28.6 ± 1.9	75.0 ± 7.0	S92	345	
12/16	6.0 ± 0.6	19.2 ± 1.9	26.9 ± 2.6	85.89 ± 13.8	S92, H	345	
01/24		17.5 ± 0.5	25.6 ± 0.7		S92	345	
01/31	5.6 ± 0.6	16.1 ± 0.3	24.0 ± 0.7	52.0 5.0	S92	345	
2/6,8							(Nebula)
02/07				40.0 ± 4.0	V	336	
02/09				40.0 ± 4.0	S92, H	345	
1993							
3/19–20							(Nebula)
03/25				28.0 3.0	V	255	
03/26				53.0 5.0	V	34	
03/29				61.0 ± 6.0	V	347	
1994							
06/20	11.4 ± 0.4	24.9 ± 1.1	30.7 ± 1.9	43.1 ± 13.3		15	
07/12							(Nebula)
09/15		20.0 ± 3.4				15	
1995							
02/19		22.3 ± 1.4	26.3 ± 1.2			345	
02/26	7.1 ± 1.2	21.5 ± 1.9	25.1 ± 2.2	65.9 ± 13.5		345	
03/14	6.3 ± 0.5	19.3 ± 1.4	24.0 ± 3.1	49.5 ± 10.2		345	
03/16	5.0 ± 0.9					345	
03/23	63.4 ± 2.9					345	9503B (S97)
03/30	89.2 ± 12.9					345	9503B
04/08	15.2 ± 0.6					345	9503B
04/15	8.6 ± 0.5	23.4 ± 1.3	28.0 ± 2.0	48.2 ± 8.1		345	
04/24	7.4 ± 0.5					345	
05/24	8.7 ± 1.7					345	
06/09	7.2 ± 0.6					15	
06/11	8.4 ± 0.7					15	
06/18	7.6 ± 0.9					15	
06/25	7.7 ± 0.4					15	
07/09	9.1 ± 0.6	23.8 ± 1.1	23.5 ± 3.0	43.5 ± 5.3		15	
07/11	9.0 ± 0.2	21.3 ± 0.8	27.5 ± 1.2	44.3 ± 2.4		15	
07/20	37.0 ± 4.0				S95	15	Tiermes (L)
07/21							(Nebula)
07/27	34.5 ± 1.9	45.3 ± 2.0	48.7 ± 3.0	59.5 ± 4.2		15	Tiermes
08/19	32.7 ± 2.0					15	Ukko + T (L)

(*continued on next page*)

Table 1 (*continued*)

Date	IR brightness (GW/(str μm))				Ref.[a]	Long.	Active volc.
	2.3 μm	3.5 μm	3.8 μm	4.9 μm			
08/26	25.7 ± 1.6	57.1 ± 2.6	63.1 ± 2.8	94.3 ± 8.3		15	Loki + TU (L)
08/28	21.4 ± 1.2	46.6 ± 4.9	85.5 ± 14.4	37.9 ± 6.4		15	Loki + TU
09/04	20.2 ± 1.3					15	Loki + TU
09/18	22.4 ± 5.4	119.3 ± 36.8	71.1 ± 21.9			15	Loki + TU
09/20	17.5 ± 1.1	45.3 ± 1.2	49.6 ± 3.5	69.0 ± 11.6		15	Loki + TU
10/05	17.0 ± 2.9	41.7 ± 4.0	40.2 ± 3.5			15	Loki
10/12	16.4 ± 1.3					15	Loki
11/12	14.5 ± 4.0	52.5 ± 6.8	60.8 ± 10.2	79.2 ± 10.2		15	Loki
1996							
02/06		44.5 ± 1.6	60.2 ± 4.3			345	Loki
02/13		28.1 ± 3.2	47.0 ± 4.9	287.5 ± 37.1		345	(Loki)
02/15	10.4 ± 1.0	32.8 ± 2.1	44.8 ± 4.0	113.4 ± 23.3		345	Loki
02/29	9.8 ± 1.2	32.8 ± 0.9	39.1 ± 1.8	104.4 ± 9.2		345	Loki
03/23	5.6 ± 0.2	27.3 ± 1.7	33.4 ± 1.8	77.7 ± 10.0		345	
04/03	4.2 ± 0.9					345	
04/08	6.5 ± 0.4	24.5 ± 1.1	28.8 ± 2.1	83.7 ± 3.8		345	
04/24	5.5 ± 0.4	22.7 ± 1.0	27.5 ± 1.0	70.9 ± 7.4		345	
04/26	4.7 ± 0.5					345	
04/26	4.9 ± 0.2	20.4 ± 0.6	21.3 ± 0.8			345	
05/28	4.6 ± 0.4					345	
06/02	5.4 ± 0.2	20.7 ± 0.6	25.3 ± 0.7	77.0 ± 8.7		345	
06/04	5.0 ± 0.7					345	
06/20	5.1 ± 0.3					345	
06/27	3.5 ± 1.2		15.7 ± 1.4			345	
08/07	7.0 ± 0.2					15	
08/12	5.6 ± 0.2	18.1 ± 1.0	20.9 ± 0.9			15	
08/14	4.7 ± 0.2	16.8 ± 0.3		65.9 ± 20.3		15	
08/23	5.4 ± 3.3					15	
08/28	33.3 ± 0.3	38.4 ± 0.4	42.0 ± 1.2	64.1 ± 6.7		15	Karei (L)
08/30	21.4 ± 0.8	30.5 ± 1.4	31.0 ± 1.1	62.9 ± 2.8		15	Karei
09/06	12.0 ± 0.2	23.6 ± 0.4	26.0 ± 1.2	57.9 ± 2.1		15	Karei
09/08	5.3 ± 0.6					15	
09/15	5.7 ± 0.7					15	
09/22	7.8 ± 0.3					15	
09/30							(Nebula)
10/01	No change				S97	15	
10/06	292.6 ± 13.2	146.0 ± 4.0	165.8 ± 3.0	111.3 ± 9.8		15	9610A (S97)
10/08	8.8 ± 0.3					15	
10/22	4.8 ± 0.3	15.6 ± 1.0	18.2 ± 1.5	43.5 ± 8.3		15	
10/31	5.8 ± 0.8					15	
11/07	3.4 ± 0.9					15	
1997							
03/12	17.0 ± 6.3	70.6 ± 2.6	80.1 ± 2.2			345	Loki (L)
03/19	19.0 ± 2.3	75.9 ± 2.8	104.6 ± 3.8	195.3 ± 8.8		345	Loki
04/20	21.0 ± 1.1	85.6 ± 5.3		250.4 ± 32.3		345	Loki
04/22	17.5 ± 0.8					345	Loki
04/29	20.6 ± 0.4	92.1 ± 2.5	110.6 ± 3.0	200.7 ± 21.0		345	Loki
05/08	22.2 ± 0.8					345	Loki
05/22	30.9 ± 11.4					345	Loki
05/24	20.4 ± 0.7					345	Loki
05/31	29.5 ± 0.8					345	Loki
06/07	206.2 ± 7.5					345	Loki +
06/14	27.2 ± 4.6					345	Loki
06/30	11.3 ± 0.2	64.3 ± 1.2	80.1 ± 1.5	160.9 ± 8.7		345	Loki
07/09	12.3 ± 1.1					345	Loki
07/23		40.6 ± 1.8	49.2 ± 2.6	173.2 ± 36.9		345	Loki
07/25	7.4 ± 1.3					345	Loki

(*continued on next page*)

Table 1 (*continued*)

Date	IR brightness (GW/(str μm))				Ref.[a]	Long.	Active volc.
	2.3 μm	3.5 μm	3.8 μm	4.9 μm			
08/01	9.8 ± 1.3					345	Loki
8/2–3							(Nebula)
08/24	7.3 ± 1.0	32.0 ± 3.3	46.5 ± 4.1	71.6 ± 7.5		15	Loki
8/29–9/2							(Nebula)
08/31	10.8 ± 0.3	29.4 ± 1.3	33.7 ± 2.1	103.4 ± 17.4		15	(Loki)
09/09	7.7 ± 0.3	27.6 ± 1.0	39.8 ± 1.1	77.0 ± 1.4		15	
09/11	8.1 ± 0.7					15	
09/18	3.6 ± 0.1					15	
09/26							(Nebula)
10/04	7.9 ± 0.4	24.9 ± 0.9	28.6 ± 1.0	70.2 ± 4.4		15	
10/11	7.2 ± 0.3	19.6 ± 0.7	37.4 ± 1.4	57.9 ± 5.1		15	
10/18	7.2 ± 0.3	24.0 ± 1.1	29.1 ± 1.3	57.9 ± 3.1		15	
10/20	5.6 ± 0.3					15	
10/25	13.9 ± 0.9	27.1 ± 4.6	39.1 ± 3.1	77.7 ± 13.1		15	
10/27	5.6 ± 0.6					15	
11/10	8.1 ± 0.5	26.6 ± 1.0	30.2 ± 1.6	74.9 ± 12.6		15	
12/28	4.5 ± 1.1	8.7 ± 0.3	14.4 ± 0.9			15	
1998–1999							
04/07		20.2 ± 3.4	17.9 ± 5.5			345	
04/09		18.4 ± 2.1	25.8 ± 6.2			345	
04/25	6.2 ± 0.3	21.9 ± 1.4	25.3 ± 1.6	66.5 ± 3.0		345	
05/02	2.2 ± 0.2	20.5 ± 1.1	25.1 ± 1.4	54.8 ± 5.3		345	
05/18	7.3 ± 0.4	23.2 ± 1.5	28.8 ± 2.1	66.5 ± 2.4		345	
05/27	17.0 ± 5.2					345	Loki
06/03	35.5 ± 8.6					345	Loki
06/10	13.6 ± 0.6	54.0 ± 1.5	64.8 ± 2.3	144.1 ± 6.5		345	Loki
06/19	14.4 ± 0.7	70.6 ± 3.2	82.4 ± 3.0	130.2 ± 14.7		345	Loki
07/28	12.8 ± 0.5	56.6 ± 1.5	66.0 ± 1.8	125.5 ± 11.0		345	Loki
08/15							(Nebula)
08/20	10.0 ± 0.3	50.2 ± 1.4	62.5 ± 1.7	149.5 ± 6.7		345	Loki
08/27	11.0 ± 0.7	53.0 ± 2.4	64.8 ± 2.9	130.2 ± 7.0		345	Loki
08/29	17.5 ± 0.8	56.6 ± 2.6	66.0 ± 3.0	150.9 ± 5.5		345	Loki
9/15–19							(Nebula)
09/30	8.8 ± 0.3	35.4 ± 1.3	43.6 ± 1.6	111.3 ± 3.0		15	Loki
10/05	8.4 ± 0.3	38.8 ± 1.7	46.1 ± 1.7	92.6 ± 19.0		15	Loki
11/29	9.6 ± 1.2	44.9 ± 6.2	52.9 ± 6.0	99.7 ± 15.2		15	Loki
12/15	28.2 ± 1.0	66.8 ± 1.8	75.8 ± 2.1	124.3 ± 5.6		15	Loki +
12/31	7.2 ± 0.3	32.0 ± 1.2	39.1 ± 1.4	97.0 ± 6.9		15	(Loki)
01/23	5.0 ± 0.4	21.7 ± 1.7	26.8 ± 3.5			15	
02/08	6.2 ± 0.3	22.3 ± 0.8	28.0 ± 1.3			15	
02/09	6.5 ± 1.8	21.3 ± 1.9	26.0 ± 2.9	89.2 ± 7.9		15	

[a] V: Veeder et al. (1994). H: Howell and Klassen (private communication, 2002). S94: Spencer et al. (1994). S92: Spencer et al. (1992). S95: Silverstone et al. (1995). S97a: Spencer et al. (1997). S97b: Stansberry et al. (1997). Unreferenced: Previously unpublished data obtained at Nasa's Infared Telescope Facility using NFSCAM. L: Lopes-Gautier (1997). T = volcano Tiermes Patera. U = volcano Ukko Patera. TU = volcanoes Tiermes and Ukko simultaneuosly. "Loki+" = possible short, unidentified eruption in addition to Loki eruption.

to categorize Io's activity level as quiet. As a result we obtain a strong lower limit to the probability that Io was in fact volcanically quiet during these nebula observations.

2.3.1. Long-term non-Loki eruptions

In 1995, Tiermes Patera and Ukko Patera erupted at detectable levels for 60–80 days and 30–70 days, respectively. Together, these represent 14 of the 23 non-Loki eruption measurements in the total dataset of 120 nights. (The eruptions overlapped in time, but we treat them as two separate eruptions for our statistics.) These two volcanoes thus represent the majority of non-Loki activity in our data; however their long duration also makes it less likely that similar eruptions could have occurred during a nebula observation without being detected in an earlier or later IR measurement.

We estimate that one or more Tiermes/Ukko-style eruptions are occurring on Io's Jupiter-facing hemisphere ∼ 8% of the time (see Appendix A), or 15% of the time globally. Assuming these types of eruptions last at least 30 days, the only opportunities for similar eruptions to affect the observed nebulas without being detected in the IR data are in 1993 and 1994. There is a 5-day gap between the nebula ob-

servation and IR observation in 1993, so a 60-day eruption has a 92% chance of being detected by the IR observation if it occurs during the nebula observation. Thus, the chance of Tiermes/Ukko-type activity during the 1993 nebula observation is ∼ 0.7% on the Jupiter-facing hemisphere of Io, or ∼ 9% globally. (The other hemisphere is never measured.) The 22-day gap between IR and nebula data in 1994 correspondingly makes for a 3% chance of an eruption occurring on the sub-jovian hemisphere during the nebula observation, or 11% globally.

2.3.2. Mid-range non-Loki eruptions

Two eruptions in the data lasted between 16 and 30 days: 9503B and 9812A. We estimate these types of eruptions happen ∼ 4% of the time on Io's Jupiter-facing hemisphere (see Appendix A), or 8% globally. As with the Tiermes and Ukko eruptions, the only significant opportunities for similar eruptions to affect nebula observations and still be undetected are in 1993 and 1994. A volcanic event of this type is most likely to have occurred during these nebula observations if we assume the minimum duration of 16 days. The result for the Jupiter-facing hemisphere of Io is a 1% chance of an eruption during the 1993 nebula and a 4% chance of an eruption for the 1994 nebula, or 5 and 8% globally, respectively.

2.3.3. Short-term non-Loki eruptions

Three eruptions in the IR data lasted less than 2 weeks: Karei in 1996 lasted 9–14 days; 9610A lasted 1–7 days; and 9706A lasted 1–14 days. Other eruptions with these durations could have occurred without detection during any of the nebula observations—most importantly, during the periods when Loki was not active. Nebula observations were made in IR data gaps of 7 days in 1992, 9 days in 1996, and 16 days in 1997.

As there are more opportunities to miss such short eruptions in the IR data gaps, we can approximately estimate their occurrence rate as the detection rate in these data. In total the three short eruptions represent 5 detections, or 4% of the IR observation days. We will therefore assume the worst case for our level of certainty—that such short-term eruptions are happening 4% of the time on Io's Jupiter-facing hemisphere, regardless of any IR observations made on previous or subsequent nights. This implies eruptions 8% of the time globally.

2.3.4. Outbursts

Outbursts are bright and short eruptions perhaps lasting less than one day. They are estimated to occur 3% of the time globally (Spencer and Schneider, 1996). The short-term eruptions considered above may or may not be outbursts, so assuming the maximum amount of doubt, we must add outbursts as a 4th type of eruption that may occur in-between IR observations. That means that, taken together, short-term eruptions and outbursts are occurring 11% of the time globally, regardless of IR data 1 day earlier or later.

Table 2
Total volcanically active contribution to "quiet" nebulas

Year	Total prob. (%)	Short + outburst (%)	Mid (%)	Long (%)
1992	22	11	4	8
1993	23	11	5	9
1994	27	11	8	11
1996	22	11	4	8
1997 Sept	22	11	4	8
Average	23			

The total probability of an eruption happening includes one or more eruption types happening simultaneously. The probability of the opposite—no eruption happening—is the product of the probabilities of no eruption for each type of eruption. For example, in 1992 the probability of no eruption is $0.89 \times 0.96 \times 0.92 = 0.78$, meaning a 22% chance of one or more eruptions happening.

To summarize the above, there is ample evidence to characterize a nebula observation as being made during volcanically-active periods. For those made during lulls in major activity, but possibly near a time of a short-term eruption, we must turn to statistical treatments to characterize a "quite-time" nebula, and these cases are summarized in Table 2.

2.4. Observational trend

In Fig. 1 we display all of the nebula images by year and group them according to their volcanic activity. Since the IR activity level crossed the active/quiet threshold during the 1997 observation period, the nebula of August 2–3 is placed in the active group, and the nebula of September 26 is placed in the quiet group. The nebula observed in-between these dates (August 29 to September 2) is not shown in Fig. 1 since the IR brightness changed from "quiet" to "active" during the 5-night observing sequence, meaning that nebula does not belong in either group.

There are significant differences in the brightness and shape of the sodium nebula images in Fig. 1 that appear to be correlated with the volcanic activity on Io. Jupiter's sodium nebula was on average ∼ 3 times brighter during volcanically active periods than during quiet periods. Although the nebulas from 1990 (active), 1991 (active), 1996 (quiet), and 1997 (both) were very similar in brightness, there was no volcanically quiet nebula that appeared brighter than any volcanically active nebula. The nebula was brightest in 1995 and 1998, which were both volcanically active periods, while it was dimmest in 1992 and 1993, which were both volcanically quiet periods. As Fig. 1 shows, the nebula's brightness contours during the volcanically active periods of 1991, 1995, and 1998 were distinctly rectangular in shape and, with the exception of the very dim appearance in 1992, the nebula lacked this rectangular shape during volcanically quiet periods.

Our attempts to correlate in a rigorously quantitative way the dual characteristics (brightness and shape) of the nebulas with Io's volcanic IR brightness levels met with mixed success. In Fig. 2, we display the sodium brightness at a fixed

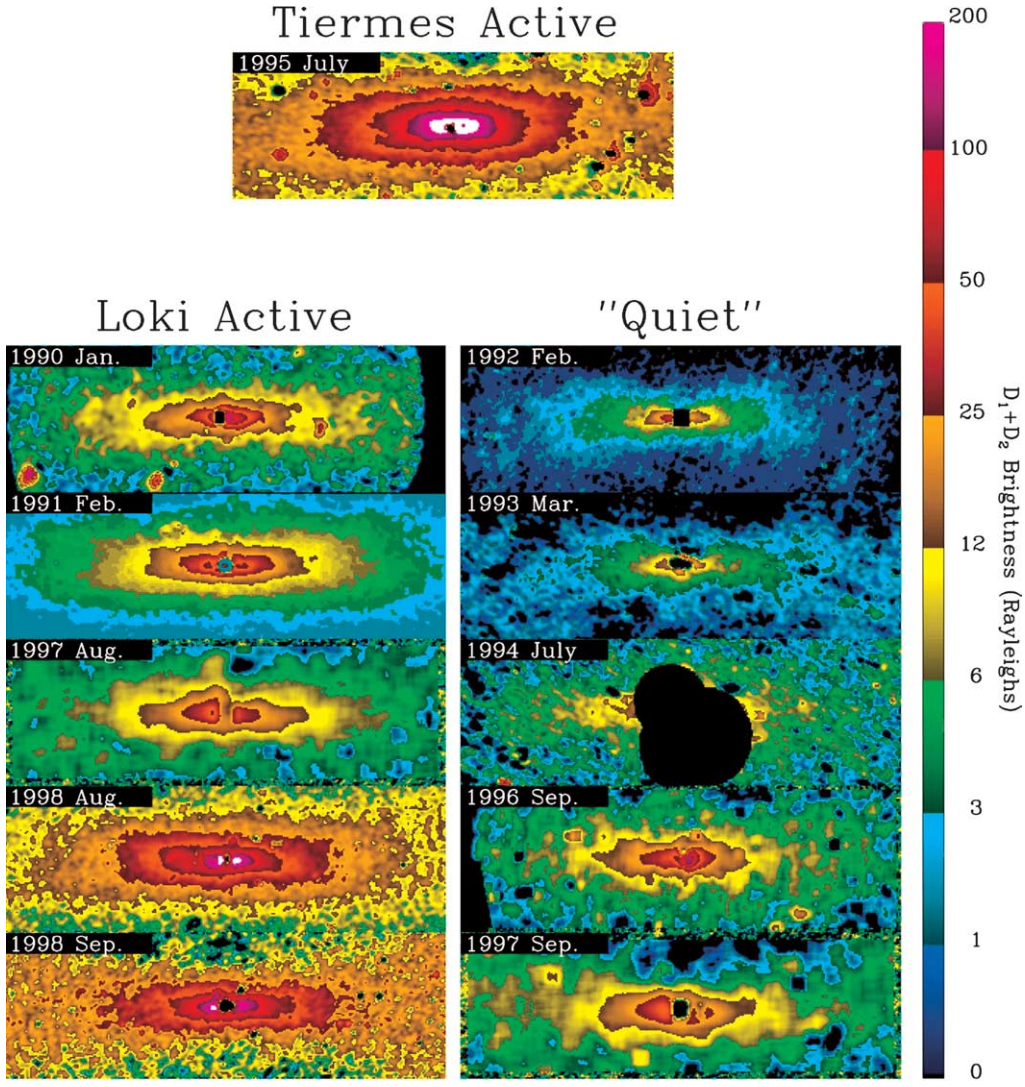

Fig. 1. Summary of Jupiter's sodium nebula and Io's volcanic activity analyses for the 9-year period 1990–1998. (Top panel) Image from 1995 taken during an eruption of Tiermes Patera. (Middle panels) Remaining nebula images sorted by Loki's volcanic activity level. Occulting masks of various sizes were used to block Jupiter and its inner moon (and especially so in the 1994 panel).

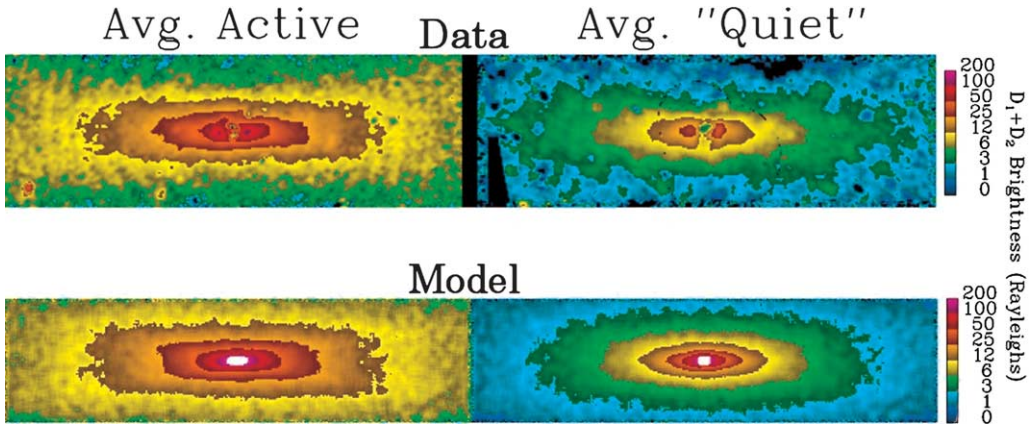

Fig. 3. (Top panels) Average of nebula images for the active (left) and quiet (right) Loki periods shown in Fig. 1. (Bottom panels) Models of the average sodium nebulas for volcanically active (left) and quiet periods (right).

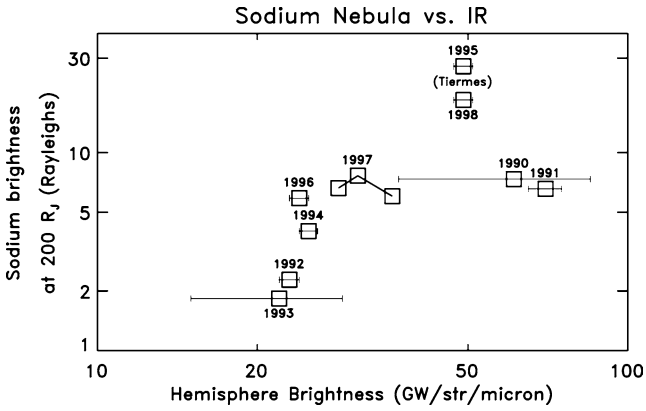

Fig. 2. Plot of Io's sub-jovian hemispheric brightness at 3.5 μm vs. the brightness of the sodium nebula at 200R_J from Jupiter. Uncertainty bars indicate the range of IR brightness measured before and after each nebula observation. The IR values and their uncertainty bars do not take into account the anti-jovian hemisphere, i.e., the possible 25% chance of an active eruption during the "quiet" nebula observations of 1992, 1993, 1994, 1996, and 1997 (dimmest value).

radial distance (200R_J) with the hemispheric brightness values "at the time of the observations" (as described above). The trend noted in Fig. 1 is again evident here. Less successful were attempts to quantify the spatial morphology of each nebula by simple parameterizations of rectangular-shaped vs. diamond-shaped brightness contour features. Thus, the trends shown in Fig. 1 and the population of only two of four possible quadrants in Fig. 2 remain as the best specifications we can offer of Io's volcanic control of Jupiter's great sodium nebula.

3. Discussion

The observed trend for the nebula to be bright and rectangular-shaped during volcanically active periods and dim and/or non-rectangular during volcanically quiet periods is most likely explained by variations in the degree of torus mass-loading by molecular ions (NaX^+). That is, the escape rate of NaX^+ from Io's atmosphere (and the resulting rate of its neutralization in the plasma torus) is higher during volcanically active periods than during volcanically quiet periods. Wilson et al. (2002) showed quantitatively how the shape and brightness of the Na nebula are, in fact, determined by the mechanism (and rate) for Na escape from Io. In Table 3 we show the results of Wilson et al. (2002), in which the same nebula images from 1990–1996 were analyzed with a neutral cloud model; also included in Table 3 are estimates of the escape rates for 1997 and 1998 based on the same model results, along with the averages for the two states of volcanic activity. The results indicate that the escape rate of NaX^+ from Io is more than four times greater during volcanically active periods than during quiet periods, implying that volcanic activity is the most important factor determining the NaX^+ escape rate. The rate of atmospheric sputtering of Na, on the other hand, does not vary as greatly,

Table 3
Sodium escape rates from Io[a] (10^{26} atoms/sec)

Volcanically active			Volcanically quiet		
Date	NaX^+	Sputter	Date	NaX^+	Sputter
1990 Jan	5.7 ± 1.6	2.0 ± 0.7	1992 Feb	2.0 ± 1.0	1.2 ± 0.6
1991 Feb	6.0 ± 1.6	1.5 ± 1.0	1993 Mar	1.8 ± 0.7	1.5 ± 1.0
1995 Jul	22 ± 8	1 ± 1	1994 Jul	2 ± 1	8 ± 3
1997 Aug[b]	4.4 ± 1.5	5.5 ± 3.5	1996 Sep	3 ± 1	9 ± 3
1998[c]	22 ± 8	1 ± 1	1997 Sep[b]	4.4 ± 1.5	5.5 ± 3.5
Average	12.0 ± 2.3	2.2 ± 0.8	Average	2.7 ± 0.5	5.0 ± 1.1

[a] Rates for 1990–1996 are taken from analyses of the same images by Wilson et al. (2002).
[b] Nebula in 1997 was similar in appearance to 1990 and 1996, so the average of 1990 and 1996 is assumed.
[c] Nebula in 1998 was similar to that in 1995, so 1995 escape rates are assumed.

and may actually be smaller during volcanically active periods. In this context, it is important to keep in mind that atmospheric sputtering rates determined from nebula images are far less certain, given the strong dependence of nebula brightness on the ejection speed of Na.

It is now possible to unify independent observations of the nebula and of volcanic activity with Monte Carlo simulations results to portray the fundamental differences in nebula brightness and appearance during volcanically active and quiet periods. We display in Fig. 3 (top panels) the averages of the observed nebula images during Loki eruptions and during quiet periods. The lower panels show the nebula model images corresponding to the average active and average quiet conditions, obtained from the simulations of Wilson et al. (2002). Given the many uncertainties in how observational components of a highly coupled system relate to parameterized simulations of it, the strong agreement displayed in Fig. 3 is both surprising and instructive.

One possible explanation for the volcanic control of the NaX^+ escape rate is that eruptions supply to Io's atmosphere a molecular sodium species (NaX) which is otherwise absent. NaX^+ can then be created by photoionization, charge exchange with torus ions (S^+, S^{++}, O^+, etc.), or electron-impact ionization. These new ions can then flow out of the ionosphere in a current, be picked up by Jupiter's magnetosphere, and later dissociated in the torus to produce the jet and stream (Wilson and Shneider, 1994, 1999) and the accompanying rectangular Na nebula (Wilson et al., 2002). Without NaX in Io's atmosphere, atomic Na^+ pickup ions can still be created, but these ions cannot form the Na stream feature due to their much longer recombination lifetimes.

Another possible explanation is that eruptions increase the density of Io's SO_2 atmosphere. NaX^+ can then be created by chemical reactions and charge exchange of torus ions with an Io atmosphere of enriched SO_2 and atomic Na (Johnson, 1994); the rates of these reactions should depend strongly on the density of Io's atmosphere and the corresponding neutral column abundances along the paths of ions traveling through the atmosphere (Wilson, 1996).

4. Summary and conclusions

We have demonstrated that Io's silicate-lava eruptions have a controlling effect on the sodium in Io's atmosphere that leads to the extended neutral Na clouds. While it is generally agreed that Io's volcanic activity is the ultimate source of Io's atmosphere, neutral clouds, and plasma torus, the firmness of our results are nonetheless somewhat unanticipated. Infrared emission from Io is a reasonable measure of lava eruptions, but we have only considered the IR brightness levels observed from half of Io's surface; we have ignored the anti-jovian hemisphere altogether (except for statistical arguments). It is the dominance of Loki, both in its IR brightness levels and apparently strong NaX output, over all of the other volcanoes that makes this possible. Loki, located on the sub-jovian hemisphere, is active approximately 50% of the time; we estimate the entire anti-jovian hemisphere to be active at most only 16% of the time. Hemispheric difference in surface and atmospheric properties are clearly important for diurnal photochemistry effects (Moses et al., 2002a, 2002b), and also in models of plume gas dynamics (Zhang et al., 2003). Such hemispheric characteristics and possible differences need to be included in future nebula source modeling.

While we retained the notation "NaX^+" to specify the unknown molecular ion containing sodium, there is considerable evidence for calling it $NaCl^+$. Observations of Cl^+ in the plasma torus (Kuppers and Schneider, 2000), direct detection of NaCl in Io's atmosphere (Lellouch et al., 2003), and a recent set of atmospheric models for volcanic conditions offer ample evidence to base further discussions upon NaCl being the parent molecule of relevance (Moses et al., 2002a, 2002b, and references therein). Atoms can be injected into Io's atmosphere by direct volcanic eruptions, by hot lava flowing over the surface causing evaporation of surface material, and by the sputtering of surface material by magnetospheric plasma. Yet, as argued by Moses et al. (2002b), molecules such as NaCl enter Io's upper atmosphere only as an unambiguous signature of very recent volcanic activity. This is a rather important result for sodium cloud physics at Jupiter, as discussed in detail by Moses et al. (2002b). While their modeling was not global or dynamical, and only specific ("Pele-type eruption") scenarios were considered, the photochemistry pointed unambiguously towards NaCl being the dominant transient in Io's upper atmosphere following large plumes. Moreover, they pointed out that NaCl is expected to be an important species for other types of plumes (Zolotov and Fegley, 2000) and that "deposits of NaCl could be vaporized by lava flowing across the surface" (Moses et al., 2002b, p. 123). The findings in our study are surely consistent with that view.

While the correlation found here applies to sodium in the atmosphere and neutral clouds, we have no observations relevant to the contributions of these lava eruptions to the more general mass budgets of S and O in the atmosphere and plasma torus. However, there is observational evidence that the sodium escape rate is indicative of S escape rates. In the only study of its kind, Brown and Bouchez (1997) monitored the brightness of the Na clouds and of the S^+ torus around Jupiter for nine months, and observed a month-long brightening in Na followed by a longer and more gradual brightening of S^+ in the torus. Unfortunately, their observational method was not able to separate the specific sodium features being monitored (i.e., "banana cloud," jet and/or stream components) and there were no data on volcanic activity during the brightening. Thus, while their increase in S^+ brightness does not necessarily represent an increase in the rate of S^+ being added to the torus, the relative timings of the Na and S^+ brightness curves are suggestive of the S^+ mass budget in the torus being somehow related to the brief increase in Na escape from Io. If the sequence observed by Brown and Bouchez is typical (S escape rates parallel Na escape rates), and if lava eruptions are the dominant means of controlling the Na escape rate from Io (meaning Brown and Bouchez's observed Na brightening was volcanically induced), then lava eruptions should affect the more general mass budget of S and O in Io's atmosphere and the plasma torus. Indeed, the recent simulations for S and O in Io's volcanically driven atmosphere (Moses et al., 2002a) are extremely interesting in this context. The dramatic differences between S/O ratios for quiescent and active times underscore the complexity of such a highly coupled and strongly driven neutral–plasma system. The recent analysis by Saur et al. (1999) for ion mass loading of the torus underscores the complexity of this process, pointing again to the need of pursuing hemispheric and time-dependent mechanisms, both observationally and via modeling. Temporal patterns and episodic morphologies are the least sampled aspects of the Jupiter–Io system. While our results are the first to relate Io's atmosphere escape and neutral cloud production to volcanic activity on Io, our limited dataset of sodium images restricts our discussion to mostly annual time scales. Brown and Bouchez (1997) were able to study shorter time scales with data on neutral and plasma conditions covering dozens of nights within a one-year period, but without the benefit of having volcanic activity indicators. It would be of great interest to obtain coordinated observations of the neutral clouds, the plasma torus, and volcanic activity on multiple nights over a span of time much less than a year.

Finally, the idea of lava flows on Io's surface having a dominant effect on Io's atmosphere is somewhat contrary to the more accepted assumption that gaseous plumes emanating from fissures on the surface are the ultimate atmospheric source. Plume eruptions do not necessarily result in increased IR flux from Io, and thus we must assume that the changing fluxes observed here are due to lava flows on the surface. It is difficult to argue against the importance of plumes to the atmosphere given their impressive size and compositional similarity to Io's atmosphere and the plasma torus. Indeed, the model results of Moses et al. (2002a, 2002b) which we have referred to repeatedly in this

work are intended for Pele-type plumes. Thus, despite the empirical evidence here linking lava flows to atmospheric escape, there is still a theoretical concern that our observed IR signatures of lava flows should have such a significant effect on the state of Io's atmosphere. However, the eruptions of Pillan in 1997 and Tvashtar in 1999/2000 have shown that lava flows and plume activity are at least sometimes correlated. This all suggests that two topics in need of further investigation are: (1) models of lava flows as a source of NaCl and other species for Io's atmosphere, and (2) observations of the sodium clouds, torus, and volcanoes on sub-annual time scales. The merging of such observations with full-system simulations will refine our understanding of how volcanoes drive the Io/Jupiter neutral clouds and subsequently all plasma populations throughout the jovian magnetosphere.

Acknowledgments

At Boston University, this work was supported, in part, by grants from the Magnetospheric Physics Program at NASA, and by seed research funds provided to the Center for Space Physics. M. Mendillo, J. Wilson, and J. Baumgardner, are guest observers at the McDonald Observatory and acknowledge the continued assistance of its director and staff. Work at Lowell is supported by grants NAG5-9004 and NAG5-10497 from the NASA Planetary Astronomy and Planetary Geology and Geophysics programs. Spencer and Stansberry are visiting astronomers at the Infrared Telescope Facility, which is operated by the University of Hawaii under agreement with NASA.

Appendix A. Patterns of volcanic activity on Io

A.1. Temporal cycles

The cycle of activity associated with the prominent volcano Loki is a well established pattern during the decade of interest to this study (Rathburn et al., 2002). Of central importance to this study, therefore, are the non-Loki events and, in particular, quiet periods. In order to rule out the occurrence of a non-Loki eruption on any particular day, IR observations both preceding and following that day are required at intervals which are smaller than the duration of the putative eruption. For instance, a series of IR observations made at 5-day intervals would detect any eruption lasting 5 days or more, but might miss eruptions lasting less than 5 days, with smaller detection probabilities for shorter eruptions.

We assume here that the durations of the known eruptions in the available IR datasets are representative of the total distribution of eruption durations on Io, and we then identify periods of time in these datasets when such eruptions can be ruled out. Thus, the estimated fraction of time when a particular type of eruption occurs, in general, is approximately the duration of the representative eruption divided by the total amount of time in the data when such an eruption could have been detected.

Table A.1
Non-Loki eruption measurements in the IR dataset

Name	# Detections	Duration (days)	Assumed duration (days)
Tiermes	8	60–85	70
Ukko	6	30–70	50
9503B	3	16–28	16 or 30
9812A	1	< 30	16 or 30
Karei	3	9–14	< 1
9610A	1	< 7	< 1
9706A	1	< 14	< 1

Table A.2
Observations that would have seen Tiermes or Ukko activity

Contiguous data windows	Tiermes start detectable	Ukko start detectable
90 days 1991–1992	160 days	140 days
270 days in 1995	340 days	320 days
270 days in 1996	340 days	320 days
240 days in 1997	310 days	290 days
300 days in 1998	370 days	350 days
Total	1520 days	1420 days
Actual eruption time	70 days	50 days
Eruption fraction	4.5% of the time	3.5% of the time

IR data from 1990 and early 1991 are not useful for this analysis, since Loki was active most of the time, and there were no regular groundbased or spacebased measurements of individual hotspots that could distinguish non-Loki emission from the main Loki eruptions. The multi-wavelength data from 1992 are useful since any eruption would be easily detected during this Loki-quiet period. Only one multi-wavelength observation is available for 1994. From 1995 onward, there are large periods of time with frequent measurements at multiple wavelengths, accompanied by observations of specific hotspots, so all of these data are useful. In the series of tables below, we summarize these findings.

A.1.1. Non-Loki events

See Table A.1.

A.1.2. Long-term eruptions of Tiermes (70 days) and Ukko (50 days)

Based on the above, we conclude that these types of eruptions are happening 8% of the time on one hemisphere, or 15% ($1.0 - [0.92 \times 0.92]$) of the time globally. See Table A.2.

A.1.3. Medium-duration eruptions 9503B and 9812A assuming 16-day eruptions

Assuming that eruptions 9503B and 9812A lasted 16 days each, for a total of 32 days of eruptions, we conclude from Table A.3 that these types of eruptions occur 3% of the time on one hemisphere or 6% of the time globally.

Table A.3
Observations that would have seen 16-day eruptions

Contiguous data windows	16-day start detectable
7 days in Nov 1991	23 days
7 days in Dec 1991	23
16 days in 1992	32
1 day in 1994	17
7 days in Feb 1995	23
40 days in Mar 1995	56
60 days in May 1995	76
55 days in Aug 1995	71
1 day in Nov 1995	17
23 days in Feb 1996	39
33 days in Mar 1996	49
30 days in May 1996	46
90 days at end of 1996	106
140 days at start of 1997	156
25 days in Aug 1997	41
36 days in Oct 1997	52
1 day in Dec 1997	17
110 days at start of 1998	126
9 days in Aug 1998	25
5 days in Sep 1998	21
1 day in Nov 1998	17
16 days in Dec 1998	32
16 days in 1999	32
Total	1097 days
Actual eruption time	32 days (16 days × 2)
Eruption fraction	3% of the time

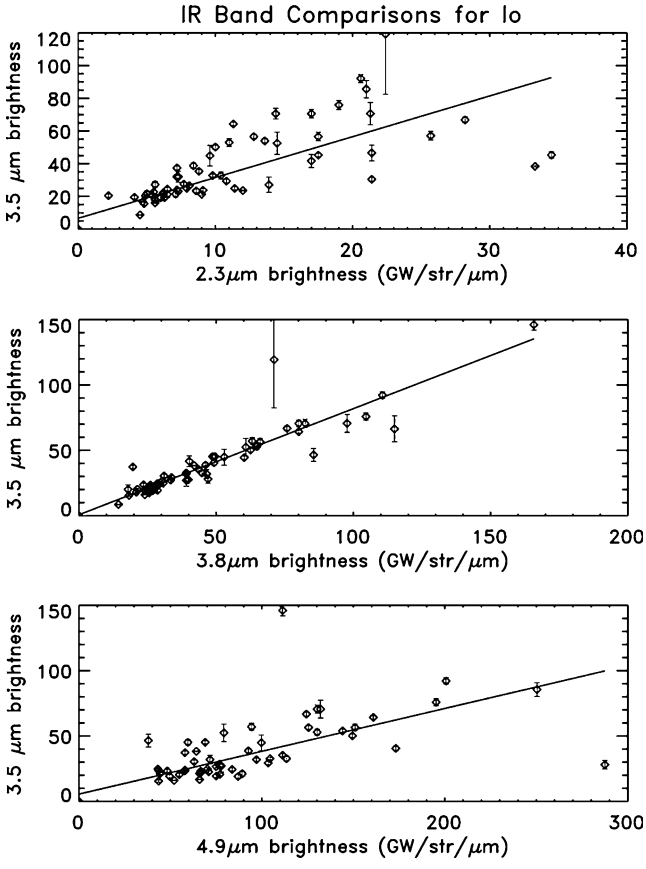

Fig. A.1. Summary of correlations of IR emissions at 2.3, 3.8, and 4.9 μm with the 3.5-μm emission.

Table A.4
Observations that would have seen 30-day eruptions

Contiguous data windows	30-day start detectable
7 days in Nov 1991	37 days
7 days in Dec 1991	37
16 days in 1992	46
1 day in 1994	31
270 days in 1995	300
140 days in early 1996	170
90 days in late 1996	120
240 days for most of 1997	270
1 day near end of 1997	31
70 days at start of 1998	100
65 days in mid 1998	95
130 days in late 1998/1999	160
Total	1397
Actual eruption time	60 days (30 days × 2)
Fraction	4% of the time

A.1.4. Medium-duration eruptions 9503B and 9812A assuming 30-day eruptions

Assuming that eruptions 9503B and 9812A lasted 30 days each, for a total of 60 days of eruptions, Table A.4 suggests that medium-range eruptions are occurring 4% of the time on one hemisphere, or 8% of the time globally. This is a higher probability, meaning more uncertainty, than the 16-day assumption, so we adopt the 30-day value.

A.2. Correlation relationships between multiple IR wavelengths

In the our main text, the summary of IR data presented in Table 1 included observations in four distinct wavelength bands. Most of our characterizations of volcanic activity used observations in the 3.5 μm band, with occasional need to use other bands when these were not available. In Fig. A.1 below, we show the correlations between the 3.5-μm brightness levels with those in the 2.3-, 3.8-, and 4.9-μm bands for the full volcanic data set. While the closely-spaced measurements at 3.5 and 3.8 μm give the best scaling patterns, the relationships with 2.3 and 4.9 μm are still useful in estimates of the 3.5-μm behavior.

References

Bagenal, F. (Ed.), 2004. Jupiter, the Planet, Satellites, and Magnetosphere. In press.

Baumgardner, J., Mendillo, M., 1993. If Galileo had a CCD. Sky Telescope 85, 19–21.

Baumgardner, J., Flynn, B., Mendillo, M., 1993. Monochromatic imaging instrumentation for applications in aeronomy of the Earth and planets. Opt. Eng. 32, 3028–3032.

Brown, M., Bouchez, A., 1997. The response of Jupiter's magnetosphere to a volcanic outburst on Io. Science 278, 268–271.

Flynn, B., Mendillo, M., Baumgardner, J., 1994. The jovian sodium nebula: two years of groundbased observations. J. Geophys. Res. 99, 8403–8409.

Johnson, R.E., 1994. Formation of Na-containing molecular ions at Io. Icarus 111, 65–72.

Kuppers, M., Schneider, M.N., 2000. Discovery of chlorine in the Io torus. Geophys. Res. Lett. 27, 513–516.

Lellouch, E., Paubert, G., Moses, J.I., Schneider, N.M., Strobel, D.F., 2003. Volcanically emitted sodium chloride as a source for Io's neutral clouds and plasma torus. Nature 42, 45–47.

Lopes-Gautier, R., Davies, A.G., Carlson, R., Smythe, W., Kamp, L., Soderblom, L., Leader, F.E., Mehlman, R., the Galileo NIMS Team, 1997. Hot spots on Io: initial results from Galileo's near infrared mapping spectrometer. Geophys. Res. Lett. 24, 2439–2442.

Mendillo, M., Baumgardner, J., Flynn, B., Hughes, J., 1990. The extended sodium nebula of Jupiter. Nature 348, 312–314.

Moses, J.I., Zolotov, M.Yu., Fegley Jr., B., 2002a. Photochemistry of a volcanically driven atmosphere on Io: sulfur and oxygen species from a Pele-type eruption. Icarus 156, 76–106.

Moses, J.I., Zolotov, M.Yu., Fegley Jr., B., 2002b. Alkali and chlorine photochemistry in a volcanically driven atmosphere on Io. Icarus 156, 107–135.

Rathbun, J.A., Spencer, J.R., Davies, A.G., Howell, R.R., Wilson, L., 2002. Loki, Io: a periodic volcano. Geophys. Res. Lett. 29. 84-1–84-4.

Saur, J., Neubauer, F.M., Strobel, D.F., Summers, M.E., 1999. Three-dimensional plasma simulation of Io's interaction with the Io plasma torus: asymmetrical plasma flow. J. Geophys. Res. 104, 25105–25126.

Schneider, N.M., Smyth, W.H., McGrath, M.A., 1989. Io's atmosphere and neutral clouds. In: Belton, M.J.S., West, R.A., Rahe, J. (Eds.), Time-Variable Phenomena in the Jovian System. In: NASA SP, vol. 494. NASA, Washington, DC, pp. 75–94.

Silverstone, M.D., Becklin, E.E., Tsetsenekos, K.L., 1995. K' photometry of Io in eclipse during 1995. Bull. Am. Astron. Soc. 27, 108–109. Abstract.

Spencer, J.R., Schneider, N.M., 1996. Io on the eve of the Galileo mission. Annu. Rev. Earth Planet. Sci. 24, 125–190.

Spencer, J.R., Howell, R.R., Clark, B.E., Klassen, D.R., O'Connor, D., 1992. Volcanic activity on Io at the time of the Ulysses encounter. Science 257, 1507–1510.

Spencer, J.R., Clark, B.E., Woodney, L.M., Sinton, W.M., Toomey, D., 1994. Io hot spots in 1991: results from Europa occultation photometry and infrared imaging. Icarus 107, 195–208.

Spencer, J.R., Stansberry, J.A., Dumas, C., Vakil, D., Pregler, R., Hicks, M., Hege, K., 1997. A history of high-temperature Io volcanism: February 1995 to May 1997. Geophys. Res. Lett. 24, 2451–2454.

Stansberry, J.A., Spencer, J.R., Howell, R.R., Dumas, C., Vakil, D., 1997. Violent silicate volcanism on Io in 1996. Geophys. Res. Lett. 24, 2455–2458.

Thomas, N., 1997. The Io plasma torus. In: Barbieri, C., Rahe, J., Johnson, T., Sohus, A. (Eds.), The Three Galileos: The Man, The Spacecraft, The Telescope. Kluwer Academic, Dordrecht, pp. 225–238.

Veeder, G.J., Matson, D.L., Johnson, T.V., Blaney, D.L., Goguen, J.D., 1994. Io's heat flow from infrared radiometry: 1983–1993. J. Geophys. Res. 99, 17095–17162.

Wilson, J.K., 1996. Io's fast sodium clouds and the escape of Io's ionosphere. Thesis. Univ. of Colorado, Boulder.

Wilson, J.K., Shneider, N.M., 1994. Io's fast sodium: implications for molecular and atomic atmospheric escape. Icarus 111, 31–44.

Wilson, J.K., Schneider, N.M., 1999. Io's sodium directional feature: evidence for ionospheric escape. J. Geophys. Res. 104, 16567–16584.

Wilson, J.K., Mendillo, M., Baumgardner, J., Schneider, N.M., Trauger, J.T., Flynn, B., 2002. The dual sources of Io's sodium clouds. Icarus 157, 476–489.

Zhang, J., Goldstein, D.B., Varghese, P.L., Gimelshein, N.E., Gimelshein, S.F., Levin, D.A., 2003. Simulations of gas dynamics and radiation in volcanic plumes of Io. Icarus 163, 182–197.

Zolotov, M.Yu., Fegley Jr., B., 2000. Eruption conditions of Pele volcano on Io inferred from chemistry of its volcanic plume. Geophys. Res. Lett. 27, 2789–2792.